Resonance Raman Spectra [and Discussion]

H. J. Bernstein and A. D. Buckingham

Email alerting service   Receive free email alerts when new articles cite this article - sign up in the box
at the top right-hand corner of the article or click **here**

To subscribe to *Phil. Trans. R. Soc. Lond. A* go to: **http://rsta.royalsocietypublishing.org/subscriptions**

Resonance Raman spectra

By H. J. Bernstein

Division of Chemistry, National Research Council, Sussex Drive, Ottawa, Ontario, Canada

Selection rules for resonance Raman spectra are given for several porphins of D_{4h} point group symmetry. A normal coordinate treatment is presented, based on a potential function for which stretching and bending force constants are related to bond lengths, and to the product of the bond lengths of the bonds defining the bending angle, respectively. The results can be correlated with the persistent frequencies observed in the resonance Raman spectra of haem proteins where the haem is an iron octa-substituted porphin.

1. Introduction

The resonance Raman effect was described in considerable detail by Placzek (1934). The intensity in the ordinary Raman effect was evaluated theoretically only for the case when the frequency of the exciting line ν_0 was very different from the frequency of the molecular absorption (ν_{rn}). According to Placzek, the intensity in the Raman effect depends on

$$\sum_r \left\{ \frac{\langle k | M_\sigma | r \rangle \langle r | M_\rho | n \rangle}{\nu_{rn} - \nu_0} + \frac{\langle k | M_\rho | r \rangle \langle r | M_\sigma | n \rangle}{\nu_{rk} + \nu_0} \right\}, \tag{1}$$

where M is the electric moment, and σ and ρ are Cartesian coordinates. It is readily seen that when the exciting frequency approaches the absorption frequency, the resonance denominator approaches zero and the intensity becomes very large.

The theory for the intensity in the resonance Raman effect grew with the improvement of the experimental data and was given by Shorygin & Ivanova (1963), Behringer & Brandmuller (1956), Behringer (1958, 1967, 1974), Albrecht (1960), Mortensen (1971), Peticolas *et al.* (1970), Jacon (1972), Inagaki *et al.* (1974), Galuzzi *et al.* (1974), Mingardi & Siebrand (1974, 1975), Mingardi *et al.* (1975) and Sufra *et al.* (1977).

Although excellent investigations (Behringer 1967; Shorygin & Ivanova 1963) of the resonance Raman effect have been made with Hg arc irradiation and photoelectric detection, the introduction of the laser made it possible to irradiate the sample so as to minimize absorption of the incident beam and then self-absorption of the scattered light. A special problem is encountered when the sample is a coloured solution or solid. Irradiation into the absorption band heats the sample and a thermal lens effect is obtained (Leite *et al.* 1964) which vitiates the experiment. Also, for highly absorbing solids and powders the sample may evaporate under normal laser power and it is necessary to reduce power or cool the sample. To some extent, use of a small-bore glass sample tube in the transverse excitation mode helps to keep the sample cooler than in the normal rectilinear mode. Use of a rotating sample holder for liquids, solutions (Kiefer & Bernstein 1971a) and powders (Kiefer & Bernstein 1971b) exposes an unheated sample to the laser beam and permits the observation of high quality resonance Raman spectra.

In the following pages we shall attempt to indicate the group theoretical procedures required

to assign observed resonance Raman spectra of model metallo-porphin compounds of various molecular point group symmetries (essentially D_{4h} and C_{4h}). The assignment is then verified and fitted by a normal coordinate treatment.

2. Vibronic theory – the excitation profile

For Raman spectra excited in the region of allowed electronic absorption bands, the vibrational modes which are expected to show intensity enhancement are those which lend intensity to the electronic spectrum. These may be of two kinds: (a) modes which connect the ground state to the excited state through Franck–Condon overlap, and (b) modes which mix at least two allowed electronic transitions. The modes of type (a) are totally symmetric while type (b) modes are usually not totally symmetric and are of any symmetry that is contained in the direct product of the representations of the two allowed electronic transitions. So, for example, if there are two transitions of E_u symmetry and the molecular point group symmetry is D_{4h}, the vibrational species which can be vibronically activated are given by the direct product:

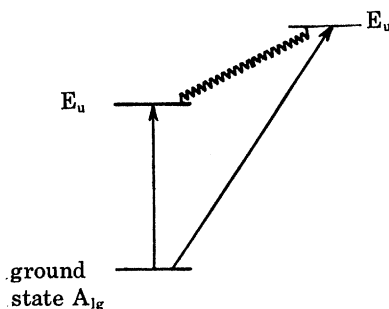$$E_u \times E_u = A_{2g} + B_{1g} + B_{2g} + A_{1g}.$$

FIGURE 1. Vibronic interaction for D_{4h} point group symmetry.

The A_{1g} modes do not participate in the vibronic coupling since they do not alter the symmetry of an interacting transition. The non-totally symmetric modes, however, of species A_{2g} and $B_{1g} + B_{2g}$ can be sufficiently intense, and even dominate the resonance Raman spectrum. In figure 1 vibronic coupling is displayed for D_{4h} symmetry.

The intensity of the scattered light depends on its frequency and on the polarizability tensor α_{ij}. For the Stokes band,

$$I \propto (\nu - \nu_R)^4 |\alpha_{ij}|^2 \tag{1}$$

where ν is the frequency of the exciting light and ν_R is the Raman shift. The intensity comes from the square of the polarizability tensor where α_{ij} is given by:

$$\alpha_{ij} = \begin{pmatrix} \alpha_{xx} & \alpha_{xy} & \alpha_{xz} \\ \alpha_{yx} & \alpha_{yy} & \alpha_{yz} \\ \alpha_{zx} & \alpha_{zy} & \alpha_{zz} \end{pmatrix}$$

and the elements α_{ij} depend in general on the frequency of the excitation.

3. THE POLARIZABILITY

In general the α_{ij} depend on the frequency of excitation and its proximity to that of the nearest allowed absorption band. The depolarization ratios also in general show either a dispersion, or a constant value, determined by the symmetry of the mode. The depolarization ratio ρ_l is given by

$$\rho_l = \frac{3\gamma_s^2 + 5\gamma_a^2}{45\overline{\alpha}^2 + 4\gamma_s^2},$$

where

$$9\overline{\alpha}^2 = (\alpha_{xx} + \alpha_{yy} + \alpha_{zz})^2,$$

$$\gamma_s^2 = \tfrac{1}{2}\{(\alpha_{xx} - \alpha_{yy})^2 + (\alpha_{xx} - \alpha_{zz})^2 + (\alpha_{yy} - \alpha_{zz})^2\}$$
$$+ \tfrac{3}{4}\{(\alpha_{xy} + \alpha_{yx})^2 + (\alpha_{xz} + \alpha_{zx})^2 + (\alpha_{yz} + \alpha_{zy})^2\},$$

and

$$\gamma_a^2 = \tfrac{3}{4}\{(\alpha_{xy} - \alpha_{yx})^2 + (\alpha_{xz} - \alpha_{zx})^2 + (\alpha_{yz} - \alpha_{zy})^2\}.$$

For the ordinary Raman effect occurring when the excitation frequency is far removed from that of the nearest absorption band the tensor is symmetric and $\alpha_{ij} = \alpha_{ji}$. Hence $\gamma_a^2 = 0$ and ρ_l has its well known form for non-resonant Raman spectra obtained with plane polarized exciting light:

$$\rho_l = 3\gamma_s^2/(45\overline{\alpha}^2 + 4\gamma_s^2),$$

with γ_s^2 as above with $\alpha_{xy} = \alpha_{yx}$ etc. It is clear then that ρ_l can have values from 0 to $\tfrac{3}{4}$ for totally symmetric modes but only $\tfrac{3}{4}$ when $45\overline{\alpha}^2$ is zero and we are concerned with non-totally symmetric modes. These are shown in table 1 in the first and second lines respectively, named class II and IV according to McClain (1971).

TABLE 1. CLASSES OF RAMAN SPECTRA BASED ON INVARIANTS AND DEPOLARIZATION RATIOS

	α^2	γ_s^2	γ_a^2	
class II	+	+	0	$\rho_l = 0\text{-}\tfrac{3}{4}$
class IV	0	+	0	$\rho_l = \tfrac{3}{4}$
class I	+	+	+	$\rho_l = 0\text{-}\infty$
class III	0	+	+	$\rho_l = \tfrac{3}{4}\text{-}\infty$
class V	0	0	+	$\rho_l = \infty$

It is readily seen from table 1 that for resonance Raman bands an antisymmetric part γ_a^2 is introduced to give three extra categories of classes:

(a) for totally symmetric modes where ρ_l can be between 0 and ∞ (class I); (b) for non-totally symmetrical modes for which ρ_l can be between $\tfrac{3}{4}$ and ∞ (class III); and (c) for non-totally symmetric modes for which $\rho_l = \infty$ (class V).

The measurement of the reversal coefficients is difficult and liable to considerable error so that if $I(\perp)$ and $I(\|)$ are measured at various exciting frequencies one can usually determine unambiguously the class in table 1 to which the mode belongs, but no separate evaluation of each of α^2, γ_s^2 and γ_a^2 is possible.

4. The form of the isotropic polarizability tensor for symmetric modes

In D_{4h} for example (McClain 1971)

$$A_{1g} = \begin{pmatrix} S_1 & 0 & 0 \\ 0 & S_1 & 0 \\ 0 & 0 & S_2 \end{pmatrix},$$

hence

$$9\bar{\alpha}^2 = (\alpha_{xx} + \alpha_{yy} + \alpha_{zz})^2 = (2S_1 + S_2)^2,$$

$$\gamma_s^2 = \tfrac{1}{2}\{2(S_1 - S_2)^2 + 0\} = (S_1 - S_2)^2,$$

and

$$\gamma_a^2 = 0.$$

The depolarization ratio is given by

$$\rho_l = 3(S_1 - S_2)^2 / \{5(2S_1 + S_2)^2 + 4(S_1 - S_2)^2\}.$$

Let $S_1/S_2 = k$ so that

$$\rho_l = 3(k-1)^2 / \{5(2k+1)^2 + 4(k-1)^2\}.$$

Then for totally symmetrical modes, the depolarization ratios are shown in figure 2 for both positive and negative k (Koningstein 1972; Udagawa et al. 1974).
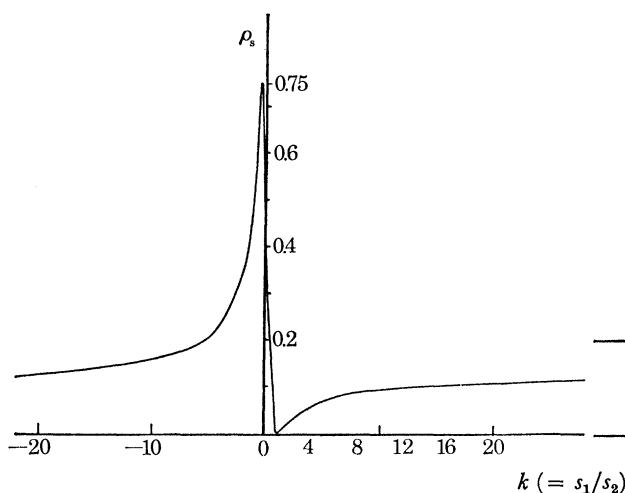

FIGURE 2. Depolarization ratios for totally symmetric modes as a function of k, the ratio s_1/s_2 in the polarizability tensor.
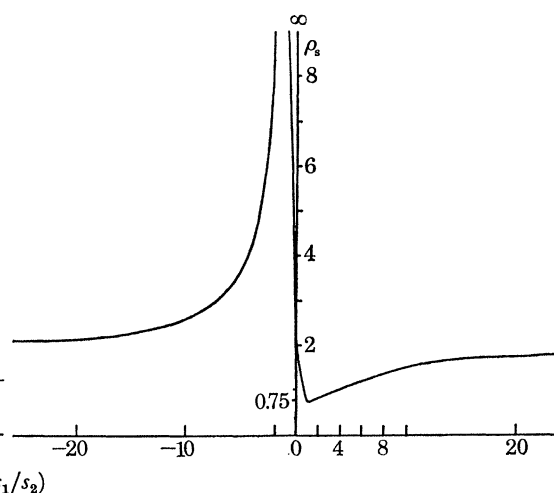
FIGURE 3. Depolarization ratios for non-totally symmetric modes as a function of k, the ratio of α_{xy} to α_{yx} of the polarizability tensor.

It is clear that if the molecule is spherical, the tensor has elements $S_1 = S_2 = S_3$, so that $\rho_l = 0$. This is the point for which $k = 1$. If, however, $S_2 = 0$ and $k = \infty$ we have a cylindrical shape for which $\rho_{k \to \infty} = \tfrac{1}{8}$. This is the value of ρ_l to be expected for disks (benzene, for example).

For only one non-zero element in the α_{ij} tensor, i.e. $k = 0$, we find $\rho_l = \tfrac{1}{3}$, which is the value expected for a diatomic species or a linear chain.

5. The form of the anisotropic polarizability tensor for non-totally symmetric modes

The polarizability tensors for B_{1g} and B_{2g} modes of D_{4h} have the form:

$$B_{1g} = \begin{pmatrix} S_3 & 0 & 0 \\ 0 & -S_3 & 0 \\ 0 & 0 & 0 \end{pmatrix} \quad \text{and evaluation of } \rho_l \text{ gives } \rho_l = \tfrac{3}{4},$$

$$B_{2g} = \begin{pmatrix} 0 & S_4 & 0 \\ S_4 & 0 & 0 \\ 0 & 0 & 0 \end{pmatrix} \quad \text{and again } \rho_l = \tfrac{3}{4}.$$

For the E_{1g} modes or $E_{1g} = \begin{pmatrix} 0 & 0 & S_5 \\ 0 & 0 & -iS_5 \\ S_6 & -iS_6 & 0 \end{pmatrix}$ and $\begin{pmatrix} 0 & 0 & S_5^* \\ 0 & 0 & iS_5^* \\ S_6^* & iS_6^* & 0 \end{pmatrix}$, where S_5^* is the complex conjugate of S_5, and

$$\rho_l = \tfrac{3}{4} + \tfrac{5}{4}(S_5 - S_6)/(S_5 + S_6)^2.$$

This is also the value for a polarizability tensor

$$\begin{pmatrix} 0 & S_5 & 0 \\ S_6 & 0 & 0 \\ 0 & 0 & 0 \end{pmatrix},$$

which occurs in the non-totally symmetric modes of the point group D_{2h}, for example. A plot of $k = S_5/S_6$ and depolarization ratio, $\rho_l = \tfrac{3}{4} + \tfrac{5}{4}(k-1)/(k+1)^2$, then shows the variety of values of ρ_l for non-totally symmetric modes of any molecular point group symmetry (figure 3). For $k = 1$ we have $\rho_l = \tfrac{3}{4}$, while for $k = -1$, $\rho_l = \infty$ as in the case of the A_{2g} modes of D_{4h} for which the tensor is

$$\begin{pmatrix} 0 & S_5 & 0 \\ -S_5 & 0 & 0 \\ 0 & 0 & 0 \end{pmatrix}.$$

Figures 2 and 3 give all the values of ρ_l uniquely determined by symmetry and independent of the frequency of the exciting line, as well as all the values expected as a function of the exciting line frequency.

In the resonance Raman effect, the A_{2g} modes of D_{4h} symmetry can dominate the spectrum so that now one expects to see modes of species A_{1g}, B_{1g}, B_{2g} and E_{1g}, and additional A_{2g} modes.

The remaining selection rules come from molecular orbital theory which indicates whether the $\pi\pi^*$ transitions give stronger vibronic coupling than the $n\pi^*$ transitions. If the planar transitions in disk-like molecules, e.g. Cu-porphin, dominate the spectrum, then the out-of-plane E_{1g} modes are very much weaker. Thus we expect only the planar A_{1g}, A_{2g}, B_{1g} and B_{2g} modes in the resonance Raman spectrum of this porphin.

It is clear that the information is of two types; one involves the fact that the intensity changes with change of frequency of the exciting line (the so-called excitation profile), and the other involves the change of ρ_l with change of frequency of the exciting line (the so-called dispersion of ρ_l). By determining the maximum in the excitation profile one can identify 0–0 and 0–1

bands in the electronic absorption spectrum for example. This was first recognized and employed by the group at the Ford laboratory (Rimai *et al.* 1971) and then by Spiro & Strekas (1972) as well as Verma & Bernstein (1974 *a*, *b*).

6. HAEM PROTEINS

The appearance of intense bands with anomalous polarization ($\rho_l > \frac{3}{4}$) (a.p.) is the most remarkable feature of haem protein spectra. Their observation (Spiro & Strekas 1972) was the first experimental confirmation of antisymmetric vibrational scattering, though the prediction was given by Placzek (1934) for the point group C_{4v}, for which the ρ_l of A_2 modes should be ∞.

For the haem proteins whose resonance Raman spectrum is dominated by the metalloporphyrin chromophore it is tempting to assume that the point group symmetry is essentially D_{4h}, and indeed in some spectra there is practically no intensity (figure 4) in the (‖) component (for the line at 1322 cm^{-1} within experimental error) and so $\rho_l \approx \infty$. However, in spectra of

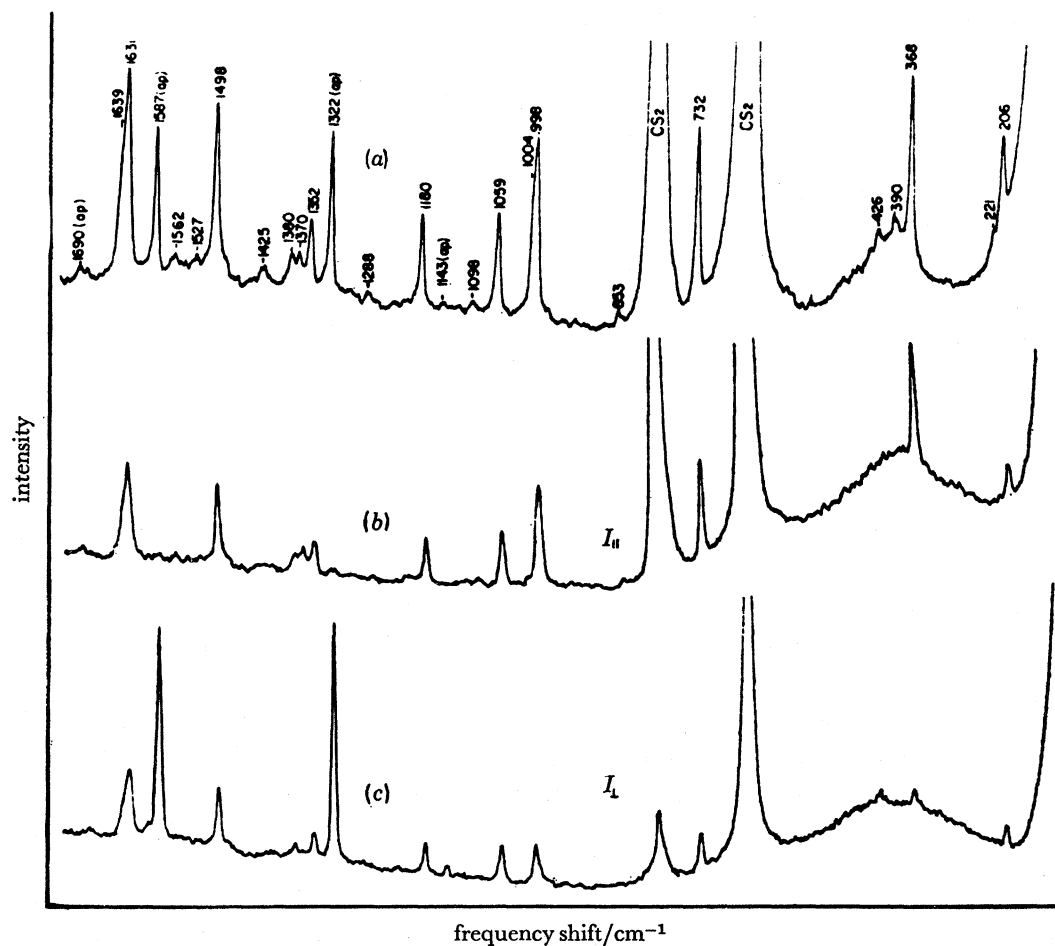FIGURE 4. Resonance Raman spectra of Cu-porphin (D_{4h}) with ($\perp$) and (‖) polarizations (Verma *et al.* 1976) 5565 Å excitation, *ca.* 5×10^{-5} M in CS$_2$ solution. Solvent lines are marked for CS$_2$. A spectrum without analyser. Bands with $\rho > \frac{3}{4}$ are marked as a.p., ($\perp$) and (‖) spectra are shown.

other haem proteins (Spiro & Strekas 1974; Verma & Bernstein 1974 a, b) the value for some of these bands is *ca.* 5 or 10 or 20. It is convenient to adopt the suggestion of Spiro & Strekas (1972) and refer to these bands as being anomalously polarized (a.p.) $\frac{3}{4} < \rho_l < \infty$, while inverse polarization (i.p.) is reserved for the case where $\rho_l = \infty$.

This observation of anomalously polarized lines gave rise to two criteria for observing the intensity of a parallel ($\parallel$) component of these a.p. modes. The obvious one is to recognize that the molecules have less than D_{4h} symmetry, but before this can be accepted one has to rule out the possibility that accidental superpositions of A_{2g} modes with A_{1g}, B_{1g} and B_{2g} modes could give a parallel component, and therefore values of ρ_l much less than ∞. In the Co-, Ni-, and Cu-mesoporphyrins ρ_l could be measured (Verma & Bernstein 1974 b) with slits of 1.5 cm^{-1} showing indeed that there are no superpositions (figure 5). To understand the spectroscopic problem completely we have obtained the spectra of some Cu porphins of chosen molecular point group symmetry listed in table 2. In figure 6 we see a resonance Raman spectrum which is by no means typical. As is apparent from the dilution, it has a smaller signal/noise ratio than could be obtained with our usual concentrations of around 10^{-4} mol cm^{-3}. The bands

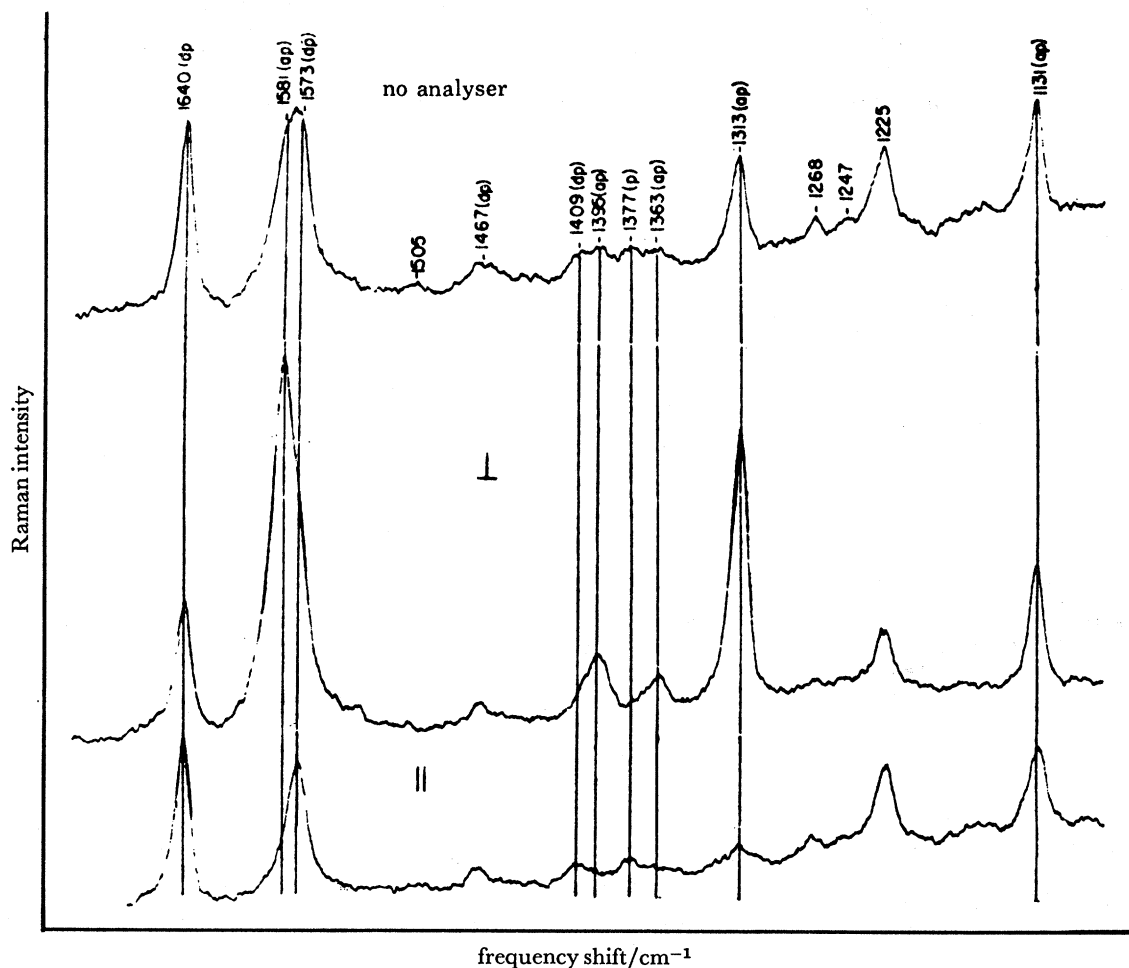FIGURE 5. Resonance Raman spectra of Cu-mesoporphyrin IX dimethylester, *ca.* 10^{-4} M in CS$_2$ solution, 5600 Å excitation. Slit width is 1.5 cm^{-1} for ρ spectrum and 2.5 cm^{-1} for bottom spectra (Mendelsohn *et al.* 1975).

TABLE 2. POINT GROUP SYMMETRIES OF CU-PORPHINS INVESTIGATED
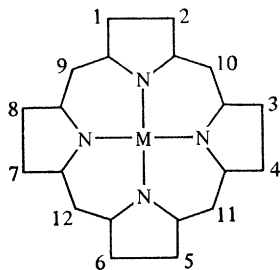
		1	2	3	4	5	6	7	8	9	10	11	12
D_{4h}	Cu-porphin	H	H	H	H	H	H	H	H	H	H	H	H
D_{4h}	Cu-porphin-d4	H	H	H	H	H	H	H	H	D	D	D	D
D_{4h}	Cu-octamethyl	M	M	M	M	M	M	M	M	H	H	H	H
D_{4h}	Cu-octamethyl-d4	M	M	M	M	M	M	M	M	D	D	D	D
C_{4h}	Cu-tetramethyl	M	H	M	H	M	H	M	H	H	H	H	H
C_{4h}	Cu-Etioporphyrin I	M	E	M	E	M	E	M	E	H	H	H	H
C_{2v}	Cu-Etioporphyrin IV	M	E	E	M	E	M	M	E	H	H	H	H
D_{2h}	Cu-Etioporphyrin II	M	E	E	M	M	E	E	M	H	H	H	H
C_{s}	Cu-Etioporphyrin III	M	E	M	E	M	E	E	M	H	H	H	H
C_{s}	Cu-meso IX	M	E	E	M	P	M	P	M	H	H	H	H

In the table, M = methyl, E = ethyl, D = deuterium, P = propionic acid.
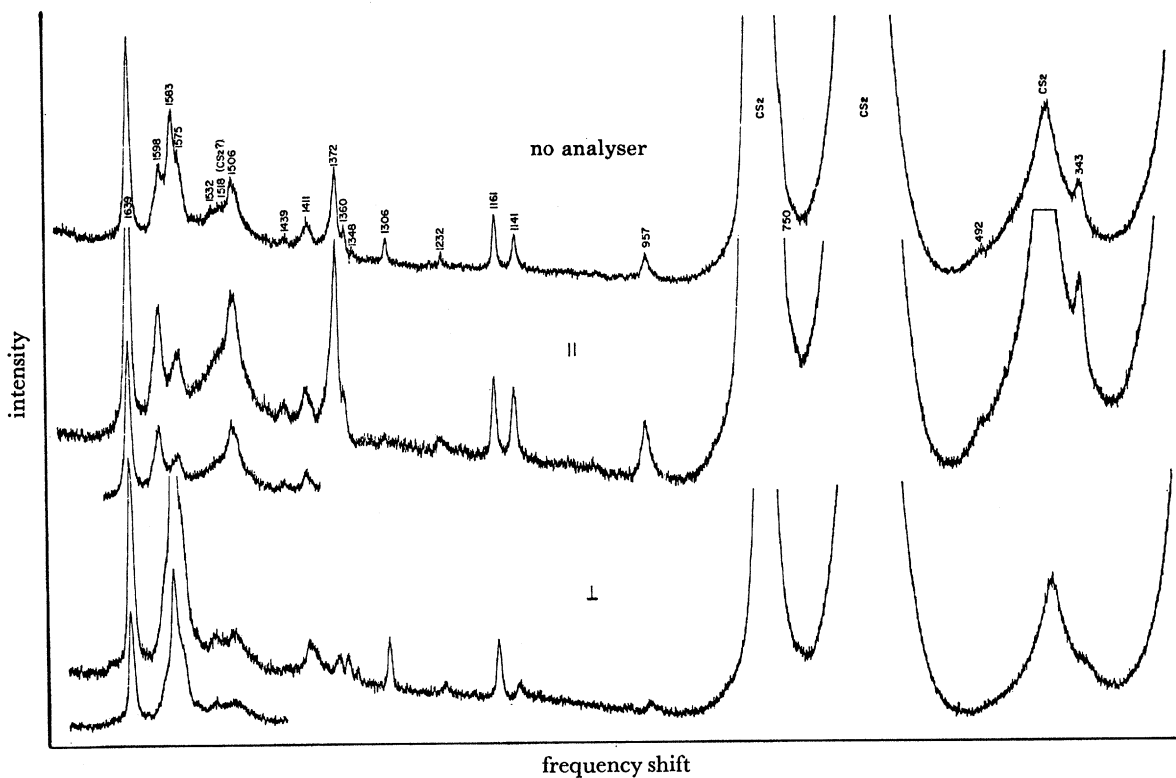
FIGURE 6. Cu-tetramethylporphin (C_{4h} symmetry).

at 1583 and 1306 cm^{-1} clearly show anomalous polarization, while bands at 1598, 1506 and 343 cm^{-1} are polarized.

Several lines were observed in these systems (Spiro *et al.* 1972) with $\rho_l \approx 5$, 10 and 30. The explanation for observing different ρ_l values instead of a constant value of ∞ may be because of overlap of two or more lines of different symmetry species. Under quite high resolution conditions, however (1.5 cm^{-1}), we observed spectra of the perpendicular and parallel components of the resonance Raman spectrum of Cu-mesoporphyrin (figure 5) and it is clear that the high and different ρ_l values really arise from well resolved lines and therefore must be attributed to lowering of the D_{4h} symmetry.
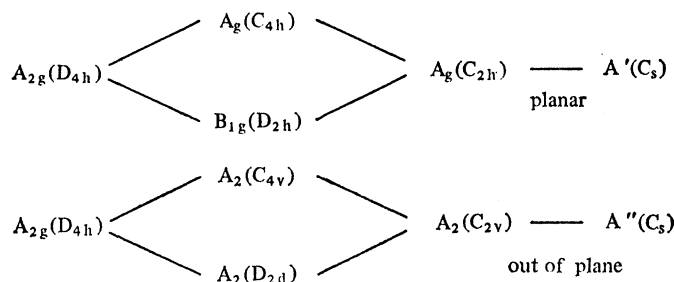

FIGURE 7. Correlation diagrams for loss of symmetry for planar and non-planar metallo-porphin.

We found Cu-porphin to be soluble in CS_2 without fluorescing (Verma *et al.* 1974). Here we have D_{4h} (rigorous) symmetry and expect also to have $9A_{1g} + 8A_{2g} + 9B_{1g} + 9B_{2g}$ Raman active modes.† The depolarization ratios should be $0-\frac{3}{4}$, for A_{1g}, ∞ for A_{2g}, and $\frac{3}{4}$ for the B_g modes. In figures 4 and 5 we see that instrumentally ∞ is to be taken at about 50. Also, if off resonance but within the band contour, the (∥) component is zero so that ρ_l is ∞ because the symmetry is still D_{4h}. Thus any value less than $\rho_l \approx 50$ is to be regarded solely as due to loss of

TABLE 3. 'EXTENDED' CHARACTER TABLE FOR THE VIBRATIONAL ANALYSIS OF THE
METALLO-PORPHINS OF D_{4h} POINT GROUP

symmetry	n	T	R	α_{ij}	ρ	vibronic	RRρ
A_{1g}	9			$XX+YY, ZZ$	$0-\frac{3}{4}$ i.p.	$E_u \times E_u$	$0-\frac{3}{4}$
A_{2g}	8		R_z	$XY-YX$	i.p.	$E_u \times E_u$	∞
B_{1g}	9			$XX-YY$	$\frac{3}{4}$ i.p.	$E_u \times E_u$	$\frac{3}{4}$
B_{2g}	9			$XY+YX$	$\frac{3}{4}$ i.p.	$E_u \times E_u$	$\frac{3}{4}$
E_g	8		R_x, R_y	$YZ\pm ZY, ZX\pm XZ$	$\frac{3}{4}$ o.p.	$E_u \times A_{2u}$	$\frac{3}{4}-\infty$
A_{1u}	[3]						
A_{2u}	6	Z			o.p.		
B_{1u}	[4]						
B_{2u}	[5]						
E_u	18	X, Y			i.p.		

[ ] not active in absorption nor Raman.
i.p. = in-plane, o.p. = out-of-plane.
T = translation.
R = rotation.
RR = resonance Raman.

† Again the A_{1g} modes are enhanced via Franck–Condon considerations and although A_{1g} is contained in the direct product $E_u \times E_u$, the A_{1g} modes are not considered to have intensity contributions resulting from this coupling.

symmetry. This can happen in several ways, for example, figure 7. Actually the correlation tables show (Mendelsohn *et al.* 1975) how two modes of A_{2g} and A_{1g} symmetries in D_{4h} become two A_g modes in C_{4h} so that observation of one of the A_g modes as resonance is reached corresponds to a high value of ρ_l, but < 50 because of the non-zero trace.

We are now in a position to summarize the information obtained from group theoretical considerations and proceed to a normal coordinate treatment. The symmetry species, number
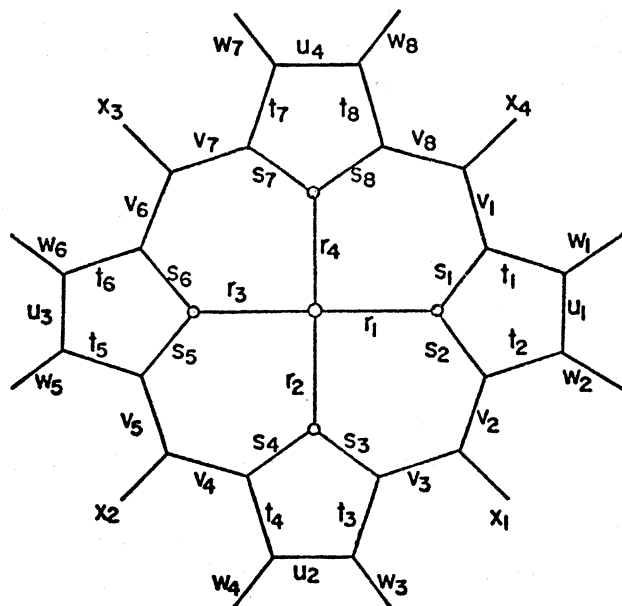

FIGURE 8. Stretching coordinates of the porphin skeleton.

TABLE 4. FORCE CONSTANTS FOR COPPER-PORPHINS

	$N\ m^{-1}$
Cu—N stretch[a]	95
C—N stretch	691
C—H stretch	512
C—C stretch[b]	478
N—Cu—N deformation[a]	14
Cu—N—C deformation[a]	50
C—C—H deformation	426
skeleton deformation[c]	102
Cu—N, Cu—N interaction	25
C—C, C—C interaction[d]	42
C—C, C—C—H interaction[e]	18
C—C, C—C—C interaction[f]	21

(*a*) These values were kept constant in the final calculation.

(*b*) This value is for the bond ab (see footnote to Table 6). Other CC stretch force constants were obtained using the k/r correlation and their respective values are bb = 687, am = 582 and the $C_b C$ methyl stretch in Cu—OMP and Cu—TMP = 408 N m⁻¹.

(*c*) This value is for $H_{(baN)}$ (see Table 6). Other skeleton deformation constants were obtained using the $d/r_1 r_2$ correlation and their respective values are MaN = 1.43, aNa = 1.51, abb = 124, ama = 137, mab = 98; and in Cu—OMP and Cu—TMP $(C_b C_b C_{methyl}) = 96$, and $(C_a C_b C_{methyl}) = 68$ N m⁻¹.

(*d*) Same value was used for $F_{CC,CN}$ and $F_{CN,CN}$. This interaction constant was used only for the stretches with a common atom.

(*e*) This interaction constant was used only for the coordinates with the common CC bond.

(*f*) Same value was used for $F_{CC,CN}$, $f_{CN|CCN}$, $f_{CN,CNC}$ and it was used only when the stretching coordinate was one of the bonds in the deformation coordinate.

of modes, components of polarizability tensor, depolarization ratio, source of vibronic activity and depolarization ratio in resonance Raman spectra are shown in table 3. It is clear that the $8A_{2g}$ modes become allowed in the resonance Raman spectrum since $\alpha_{xy} = -\alpha_{yx}$.

Before embarking on a normal coordinate treatment it is clear from figure 8 that there are not enough data to determine the stretching constants and bending force constants of a general quadratic force field. Some drastic assumptions are required to make the calculation viable. We have proceeded along the lines that the observed bond distances include effects from long-range interactions represented by the molecular orbitals used to calculate them. A one-to-one correspondence of bond stretching force constant with its internuclear distance would then be expected to take into account the delocalization effects.

TABLE 5. Cu-OCTAMETHYL, Ni-OCTAETHYL-PORPHINS AND THE SPECTRA OF FERRICYTOCHROME c AND THE PERSISTENT MODES OF HAEM PROTEINS

		Cu-octamethyl-porphin		Ni octacthyl		ferri-cytochrome c		haem proteins
		calc[a]	obs[b]	calc[g]	obs[c]	cos[d]	obs[e]	obs[f]
A_{1g}	bs	1076	1060	1039	1025			1088
	mH	3075						
	aN	1624	1598	1605	1602	1595	1592	1605, 1622
	bb	1532	1506	1526	1519	1500	1497	1480, 1510
	am	1386	1372	1380	1383	1362	1362	1360, 1373
	cbs	264	257	238	226		270	
	ab	878		805	806		871	915
	ring	661	684	658	674		692	675
	MN	357	343	362	364		350	353
A_{2g}	bS	1318	1306	1299	1309	1310	1315	1310, 1342
	aN, am	1600	1583	1602	1603	1585	1583	1585, 1553
	ab	1488	1411	1407		1400	1403	1412
	cbs	295		309				
	amH	1085	1127	1103			1130	1130
	bs, aN, am	986	995?	O				
	ring	759		783	795		752	
	ring	561		528	ca. 600			572?
B_{1g}	bs	1077	955	O			970	
	am	1578	1575	1659	1576			1560
	aN, am	1547	1555	1561		1547	1547	1547, 1552
	bb	1458	1467	1408		1404		1399
	amH	1177	1161	1237	1159		1175	1175
	cbs	322		350	344			
	ab	718	755	748	784			755
	ring	692	716	660	751			
	MN	185	172	221	226			
B_{2g}	mH	3072						
	bs	1190	1232	1182	1220	1228	1230	1225
	aN	1619	1639	1483	1655	1626	1612	1640, 1610
	ab	1441	1439	1402		1476	1387	1430
	cbs	519	492	529	496			
	am	1094	1140	1041			1086	1088
	ring	820	803	859	850		801	801
	ring	226	251	218				
	MNa	174	172	167				

(a) Sunder & Bernstein (1975 a); (b) Sunder & Bernstein (1975 b); (c) Kitagawa *et al.* (1976 a); (d) Spiro & Strekas (1972); (e) Friedman & Hochstrasser (1973); (f) Spiro & Strekas (1974); Friedman & Hochstrasser (1973); (g) Calculated in Kitagawa *et al.* (1976); O Not calculated in this approximation.
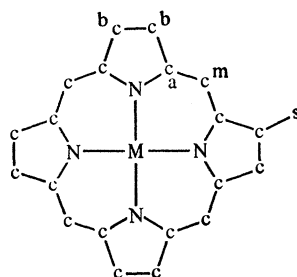
Lennard-Jones (1937) and Coulson & Longuet-Higgins (1947) obtained from molecular orbital theory a relation between bond distance and bond order for these delocalized bonds in conjugated hydrocarbons. Also, there is a relation between force constant, k, and bond order. Elimination of the bond order from these equations is expected to give a relation between k and r. Thus the C—C bond stretching constants used here were obtained by assuming they were proportional to the bond distance (Ogoshi *et al.* 1972). The proportionality constant was determined from the least squares minimization. For these molecules and skeletal angle deformation constants have also been correlated with the product of the bond distances of the bonds containing the angle. Although there is no simple theoretical justification for this as there is for the C—C bonds one does obtain a rough correlation. The calculations were made by the method of Schachtschneider (1964) and the results were obtained with the parameters shown in table 4. For the methyl-substituted compounds the CH₃ groups were replaced by a point of mass 13 at C_α. Some 140 frequencies were calculated for deuterium and methyl substituted Cu-porphins and the agreement between the observed (Verma *et al.* 1976; Sunder *et al.* 1975; Sunder & Bernstein 1975 *b*) and calculated results is about 2.5 %. In table 5 the results calculated for Cu-octamethyl and Ni-octaethyl porphin are given and, for comparison, those observed for ferrocytochrome *c*, and the average persistent frequencies of some haem proteins. It is clear that the calculated spectra show a good one-to-one correspondence with the values found in the haem proteins. Note that the inversely polarized feature at *ca.* 1310 cm⁻¹, arising from the α carbons in the pyrrole ring, is indeed a persistent mode. The potential energy distribution shows that the modes are very mixed in character, so that even approximately labelling the character of the modes as arising from a particular bond is just as a convenience and has little physical meaning. One can find modes with considerable CN content which should be metal sensitive, and indeed this is found to be the case (Sunder & Bernstein 1975 *b*). For example, the highest B_{2g} mode around 1640 cm⁻¹ depends considerably on the nature of the metal (Susi & Ard 1977).

In table 6 the calculated results for Cu-porphin, Cu-porphin-d_4, Cu-octamethyl porphin (D_{4h}) and Cu-1,3,5,7tetramethyl porphin (C_{4h}) are listed. An approximate description of the mode is also given. It is clear that a satisfactory correlation is obtained.

In table 7 the values of the frequencies calculated for Cu-porphin are compared for various potential functions of different authors. It is seen that the statistical spectrum estimated by the arithmetic mean of the calculated values indeed gives a very close picture of the spectrum of this metallo-porphin. Further, our calculated result differs from the others chiefly in the value of the highest allowed skeletal mode which we attribute primarily to the use of a high CN force constant. Also our potential function has only 12 independent parameters whereas those used by others have at least 18.

In table 8 the persistent haem protein spectra are shown and compared with the calculated octamethyl spectrum. The underlined modes are observed in the haem spectra and, where doubly underlined, there are two close-lying modes observed in the haem protein spectra. Other correlations with valence state of the Fe, and whether the Fe is low or high spin, have also been made (Spiro *et al.* 1974).

Table 6. Calculated spectra of Cu-porphin, Cu-porphin-d_4
Cu-octamethyl-porphin and Cu-tetramethyl-porphin

		Cu-porphin (D$_{4h}$)		Cu-porphin-d_4 (D$_{4h}$)		Octamethyl (D$_{4h}$)		tetramethyl (C$_{4h}$)	
		calc.	obs.	calc.	obs.	calc.	obs.	calc.	obs.
A$_{1g}$	bH/bs	3075		3074		1073	1060e	1076	1023
	mH/mD	3072		2291		3075		3072	
	aN	1624		1607		1624	1598	1628	1642
	bb	1511	1562	1511	1551	1532	1506	1520	1561
	am	1343	1370	1339	1371	1386	1372	1370	1382
	δ(bH)/δ(cbs)	1078	1065	1078	1074	264	257	266	251
	ab	999	998	989	993	878		909	889
	ring def.	742	732	723	708	661	684e	659	
	MN	360	368	359	365	357	343	356	348
A$_{2g}$	bH/bs	3071		3071		1318	1306	3074	
	am, aN	1594	1587	1594	1575	1600	1583	1595	1584
	ab	1449	1425e	1430		1488	1411	1461	1479
	δ(bH)/δ(cbs)	1304	1322	1290	1258	295		1283	1332
	δ(mH)/δ(mD)	1103	1143	823	780	1085	1127	1133	1128
	aN, am, bs	1021	1008	1054	1027	986	995?	1012	990
	ring def.	740	802	721		759		742	742
	ring def.	557	498	543		561		583	629
B$_{1g}$	bH/bs	3075		3074		1077	955	3072	
	am	1575	1631	1570		1578	1575	1571	1595
	aN	1529	1498	1523	1496	1557	1555e	1538	1507
	bb	1428	1380	1428	1380	1458	1467	1447	
	δ(mH)/δ(mD)	1153	1180e	883		1177	1161	1176	
	δ(bH)/δ(cbs)	1076	1059e	1076	1020e	322		235	
	ab	948	1004e	984		718	755e	936	918e
	ring def.	690		615	668	692	716e	694	748
	MN	224	221	224	221	185	172	217	203
B$_{2g}$	mH/mD	3073		2290		3072		3074	
	bH/bs	3070		3071		1190	1232	1163	1226
	aN	1604	1639	1592	1622	1619	1639	1612	1638
	ab	1405	1352	1404	1350	1441	1439e	1410	1352
	δ(bH)/δ(cbS)	1204	1180	1201	1208e	519	492e	1111	
	am	1081	1059e	1055	1020e	1094	1140	1081	1046
	ring def.	878	853e	874		820	803e	680	
	ring def.	410	426	409		226	251e	516	486
	δ(MNa)	216	206	213	204	174	172	177	179

TABLE 6 (*cont.*)

		Cu-porphin (D$_{4h}$)		Cu-porphin-d_4 (D$_{4h}$)		Octamethyl (D$_{4h}$)		tetramethyl (C$_{4h}$)	
		calc.	obs.	calc.	obs.	calc.	obs.	calc.	obs.
E$_u$	mH/mD	3072	3025	2290	2260^d	3072		3072	
	bH/bs	3075	3125^e	3075	3110^d	1253	1228	3072	
	bH/bs	3070	3025	3071	3046^d	1040		1137	1168
	aN	1618	1655	1507	1655	1628	1635	1623	1638
	am	1567	1567	1562	1555	1579		1571	1575
	aN	1526	1534	1519	1530	1533	1520	1527	1543
	bb	1456	1450	1448	1445	1492	1474	1472	1468
	ab	1371	1387	1370	1385	1415	1399	1385	1399
	δ(bH)/δ(cbs)	1241	1310	1223	1310	355	348	1233	1240
	δ(mH)/δ(mD)	1129	1151	862	858	1109	1149	1088	1065
	δ(bH)/δ(cbs)	1078	1057	1082	1060	296	318	360	338
	am, aN	1052	1057	1068	1060^e	1040	1091^e	1043	1027
	ab	961	998	963	994^e	884	902^e	928	889
	ring def.	838	848	831	852	724	724	755	750
	ring def.	701	702	645	638	622	611	615	634
	ring def.	426	396	421	390	552	502	533	
	ring def.	364	346	362	328	253	264	256	252
	MN	231	234	231	232	177	194	192	178

TABLE 7. COMPARISON OF THE CALCULATED SPECTRUM OF Cu PORPHIN

Cu-porphin

	(1)	(2)	(3)	(4)	(5)	(6)	(7)	(8) obs.
A$_{1g}$	1562	1624	1709	1623	1605	1600	1620±43	
	1397	1511	1581	1515	1526	1395	1487±61	
							1533±26	1562
	1335	1343	1378	1340	1330	1363	1348±15	1370
	1092	1078	1101	1036	1039	1106	1075±25	1065
	1034	999	1002	965		698	940±93	
							1000±18†	998
	700	742	712	761		619	707±38	
							729±23	732
	344	360	352	330		316	340±14	368
A$_{2g}$	1584	1594	1598	1678	1602	1610	1611±22	1587
	1305	1449	1480	1474	1407	1409	1431±37	1425
	1320	1304	1353	1314	1299	1360	1325±21	1322
	1123	1103	1150	1159	1103	1180	1136±25	1143
	929	1021	1064	1009		820	969±75	
							1006±38	1008
	755	740	786	674		695	730±38	
							760±17	802
	482	557	479	557		368	489±55	
							519±36	498
B$_{1g}$	1637	1575	1678	1701	1659	1677	1655±32	1631
	1488	1529	1651	1519	1561	1545	1549±40	
							1528±18	1498
	1336	1408	1377	1444	1408	1344	1387±34	1380
	1185	1153	1184	1243	1237	1207	1202±28	1180
	1090	1076	1101	1028		1096	1078±21	1159
	1020	948	976	986		780	942±108	1004
							983±20	
	747	690	777	723		559	700±100	
							734±25	
	251	224	217	230		258	229±12	
							222±6	221

TABLE 7. (Cu-porphin *cont.*)

B_{2g}	(1)	(2)	(3)	(4)	(5)	(6)	(7)	(8) obs.
	1451	1604	1553	1586	1483	1470	1524 ± 56	1639
	1332	1405	1535	1402	1402	1422	1408 ± 5	1352
	1177	1204	1204	1168	1182	1243	1196 ± 21	1180
	1032	1081	1055	1126	1041	858	$1032 \pm$	
							1067 ± 30	1159
	798	878	932	769		650	844 ± 60	853
	400	410	433	521		426	417 ± 12	426
	204	216	149	208		107	209	206

(calc) for Cu-porphin

E_u	(4)	(6)	(2)	(3)	a.m. (7)
	3076		3075	3096	3082
	3063		3072	3096	3077
	3061		3070	3024	3052
	1691	1652	1618	1694	1664 ± 28
	1605	1575	1567	1636	1596 ± 25
	1500	1448	1526	1555	1507 ± 34
	1482	1408	1456	1509	1464 ± 32
	1376	1340	1371	1395	1370 ± 15
	1267	1310	1241	1276	1274 ± 20
	1155	1180	1129	1159	1156 ± 14
	1080	1103	1078	1101	1091 ± 12
	1027	833	1052	1060	1046 ± 13
	966	770	961	996	974 ± 14
	789	645	838	858	828 ± 36
	695	631	701	752	716 ± 24
	422	460	426	393	426 ± 18
	369	330	364	359	356 ± 12
	244	236	231	233	236 ± 4

† The second line in column headed (7) is the arithmetic mean after deletion of the results from column (6).
(1) Solovyov *et al.* (1977); (2) Sunder & Bernstein (1975 b); (3) Susi & Ard (1977); (4) Ogoshi *et al.* (1972); (5) Kitagawa *et al.* (1976 a); (6) Warshel (1975, private communication); (7) Arithmetic mean, a.m.; (8) Verma *et al.* (1976).

TABLE 8. FREQUENCY DISTRIBUTION FOR METALLIC OCTA-SUBSTITUTED
PORPHINS AND HAEM PROTEINS (AS D_{4h})

Approximate frequency distribution for metallo-octa-substituted
porphyrins and haem proteins (as D_{4h})

A_{1g}	250, 350	670, 840	1050, 1375, 1510, 1600
A_{2g}	300	550, 800, 950	1130, 1310, 1410, 1585
B_{1g}	170, 320	730, 780	970, 1160, 1400, 1550, 1600
B_{2g}	160, 260	500, 825	1090, 1210, 1410, 1630

The work described here was done by Dr M. Asselin, Dr R. Mendelsohn, Dr S. Sunder and Dr A. L. Verma. The first calculations were performed by M. Asselin and K. G. Kidd, and performed in their final form by S. Sunder.

REFERENCES (Bernstein)

Albrecht, A. C. 1960 *J. chem. Phys.* **33**, 156.
Albrecht, A. C. 1961 *J. chem. Phys.* **34**, 1476.
Behringer, J. & Brandmuller, J. 1956 *Z. Elektrochem.* **60**, 643.
Behringer, J. 1958 *Z. Elektrochem.* **62**, 544, 900.

Behringer, J. H. 1967 *Z. Elektrochem.* **62**, 906.
Behringer, J. 1974 *J. Raman Spectrosc.* **2**, 275.
Coulson, C. A. & Longuet-Higgins, H. C. 1947 *Proc. R. Soc. Lond.* A **191**, 39.
Friedman, J. M. & Hochstrasser, R. M. 1973 *Chem. Phys.* **1**, 457.
Galuzzi, F. 1974 *J. Raman Spectrosc.* **2**, 351.
Gordon, J. F., Leite, R. C. C., Moore, R. S., Porto, S. P. S. & Whinnery, J. R. 1965 *J. appl. Phys.* **36**, 3.
Hull, R. J., Kelley, P. L., Carman, R. L. 1970 *Appl. Phys. Lett.* **17**, 539.
Inagaki, F. 1974 *J. molec. Spectrosc.* **50**, 286.
Jacon, M. 1972 *Adv. in Raman Spectrosc.* (ed. J. P. Mathieu) **1**, 324.
Kiefer, W. & Bernstein, H. J. 1971a *J. appl. Spectrosc.* **25**, 400.
Kiefer, W. & Bernstein, H. J. 1971b *J. appl. Spectrosc.* **25**, 609.
Kitagawa *et al.* 1976a *J. phys. Chem.* **60**, 1181.
Kitagawa *et al.* 1976b *Chem. Lett.* p. 249.
Koningstein, J. A. 1972 *Introduction to the theory of the Raman effect*, Dordrecht: D. Reidel.
Koningstein, J. A. & Jakubinek, B. G. 1974 *J. Raman Spectrosc.* **2**, 317.
Labeke, D. Van, Jacon, M. & Bernard, L. 1973 *Cr. hebd. Séanc. Acad. Sci., Paris* **277**B, 293, 477.
Labeke, D. Van, Jacon, M., Berjot, M. & Bernard, L. 1974 *J. Raman Spectrosc.* **2**, 219.
Leite, R. C. C., Moore, R. S. & Whinnery, J. R. 1964 *Appl. Phys. Lett.* **5**, 141.
Leite, R. C. C., Porto, S. P. S. & Damen, T. C. 1967 *Appl. Phys. Lett.* **10**, 100.
Lennard-Jones, J. E. 1937 *Proc. R. Soc. Lond.* A **138**, 280.
McClain, W. M. 1971 *J. chem. Phys.* **55**, 2789.
Mendelsohn, R., Sunder, S., Verma, A. L. & Bernstein, H. J. 1975 *J. chem. Phys.* **62**, 37.
Mingardi, M. & Siebrand, W. 1974 *Chem. Phys. Lett.* **24**, 492.
Mingardi, M. & Siebrand, W. 1975 *J. chem. Phys.* **62**, 1074.
Mingardi, M., Siebrand, W., Labeke, D. Van & Jacon, M. 1975 *Chem. Phys. Lett.* **31**, 208.
Mortensen, O. 1971 *J. molec. Spectrosc.* **39**, 48.
Mortensen, O. 1975 *Chem. Phys. Lett.* (In the press.)
Nafie, L. A., Pezolet, M. & Peticolas, W. L. 1973 *Chem. Phys. Lett.* **20**, 563.
Ogoshi, H., Saito, Y. & Nakamoto, K. 1972 *J. chem. Phys.* **57**, 4194.
Peticolas, W. L., Nafie, L., Stein, P. & Fanconi, B. 1970 *J. chem. Phys.* **52**, 1576.
Placzek, G. 1934 *Handbuch der Radiologie* VI, **2**, 209.
Rimai, L., Heyde, M. E., Heller, H. C. & Gill, D. 1971 *Chem. Phys. Lett.* **10**, 207.
Schachtschneider, J. H. 1964 Tech. Rep. 57–65, 231–64, Shell Development Co., Emeryville, California, U.S.A.
Shorygin, P. P. & Ivanova, T. M. 1963 *Optika Spektrosk.* **15**, 176.
Shriver, D. F., & Dunn, J. B. R. 1974 *J. appl. Spectrosc.* **28**, 319.
Solovyov, K. N. 1977 XIII *International Symposium on molecular spectroscopy*, Wroclaw, Poland.
Spiro, T. G. & Strekas, T. C. 1972 *Proc. natn. Acad. Sci. U.S.A.* **69**, 2622.
Spiro, T. G. & Strekas, T. C. 1974 *J. Am. chem. Soc.* **96**, 338.
Strekas, T. C., Packer, A. J. & Spiro, T. G. 1973 *J. Raman Spectrosc.* **1**, 197.
Sufra, S. 1977 *J. Raman Spectrosc.* **6**, 267.
Sunder, S. & Bernstein, H. J. 1974 *Can. J. Chem.* **52**, 2851.
Sunder, S. & Bernstein, H. J. 1975a *J. chem. Phys.* **62**, 37.
Sunder, S. & Bernstein, H. J. 1975b *J. Raman Spectrosc.* **5**, 351.
Sunder, S., Mendelsohn, R. & Bernstein, H. J. 1975 *J. chem. Phys.* **63**, 573.
Susi, H. & Ard, J. S. 1977 *Spectrochim. Acta* **33**A, 561.
Udagawa, Y., Iijima, M. & Ito, M. 1974 *J. Raman Spectrosc.* **2**, 313.
Verma, A. L., Mendelsohn, R. & Bernstein, H. J. 1974 *J. Raman Spectrosc.* **4**, 295.
Verma, A. L. & Bernstein, H. J. 1974a *J. Raman Spectrosc.* **2**, 163.
Verma, A. L. & Bernstein, H. J. 1974b *J. chem. Phys.* **61**, 2560.
Verma, A. L., Asselin, M., Sunder, S. & Bernstein, H. J. 1976 *J. Raman Spectrosc.* **4**, 295.
Woodward, W. H. & Spiro, T. G. 1974 *J. appl. Spectrosc.* **25**, 609.

Discussion

A. D. BUCKINGHAM, F.R.S. It is clear that the resonance Raman technique can have high sensitivity. It would be of interest to know how this sensitivity compares with that of other techniques such as electron spin resonance.

H. J. BERNSTEIN. The resonance Raman technique is comparable in sensitivity to that of electron spin resonance.